Environ Sci Pollut Res (2014) 21:11116–11125
DOI 10.1007/s11356-014-2515-6

Continuous flow photo-Fenton treatment of ciprofloxacin in aqueous solutions using homogeneous and magnetically recoverable catalysts

Maria J. Lima · M. Enis Leblebici · Madalena M. Dias · José Carlos B. Lopes · Cláudia G. Silva · Adrián M. T. Silva · Joaquim L. Faria

Received: 31 October 2013 / Accepted: 23 December 2013 / Published online: 23 January 2014

Abstract The degradation of ciprofloxacin was studied in aqueous solutions by using a continuous flow homogeneous photo-Fenton process under simulated solar light. The effect of different operating conditions on the degradation of ciprofloxacin was investigated by changing the hydrogen peroxide (0–2.50 mM) and iron(II) sulphate (0–10 mg Fe L^{-1}) concentrations, as well as the pH (2.8–10), irradiance (0–750 W m^{-2}) and residence time (0.13–3.4 min) of the process. As expected, the highest catalytic activity in steady state conditions was achieved at acidic pH (2.8), namely 85 % of ciprofloxacin conversion, when maintaining the other variables constant (i.e. 2.0 mg L^{-1} of iron(II), 2.50 mM of hydrogen peroxide, 1.8 min of residence time and 500 W m^{-2} of irradiance). Additionally, magnetite magnetic nanoparticles (ca. 20 nm of average particle size) were synthesized, characterized and tested as a possible catalyst for this reaction. In this case, the highest catalytic activity was achieved at natural pH, namely a 55 % average conversion of ciprofloxacin in 1.8 min of residence time and under 500 W m^{-2}. Some of the photocatalytic activity was attributed to Fe^{2+} leaching from the magnetic nanoparticles to the solution.

Responsible editor: Philippe Garrigues

M. J. Lima · C. G. Silva · A. M. T. Silva (✉) · J. L. Faria
LCM–Laboratory of Catalysis and Materials–Associate Laboratory LSRE/LCM, Faculdade de Engenharia, Universidade do Porto, R. Dr. Roberto Frias s/n, 4200-465 Porto, Portugal
e-mail: adrian@fe.up.pt

M. E. Leblebici · M. M. Dias · J. C. B. Lopes
LSRE–Laboratory of Separation and Reaction Engineering–Associate Laboratory LSRE/LCM, Faculdade de Engenharia, Universidade do Porto, R. Dr. Roberto Frias s/n, 4200-465 Porto, Portugal

Keywords Photo-Fenton · Continuous flow · Antibiotics · Ciprofloxacin · Magnetic nanoparticles

Introduction

The low biodegradability and generalized use of pharmaceutical and personal care products (PPCPs) boosted the interest on finding environmentally friendly technologies to treat waste waters containing this specific class of contaminants (Onesios et al. 2009; Yu et al. 2006). Antibiotics are PPCPs of major concern and, due to the increasing bacterial resistance to this class of drugs, public health may recede in the coming years to stages equivalent to those of pre-penicillin (Baquero et al. 2008; Batt et al. 2006; Kolpin et al. 2002). Specifically, ciprofloxacin (CIPRO) is a broad-spectrum synthetic antibiotic (a second generation fluoroquinolone) widely employed for the treatment of bacterial infections (Oliphant and Green 2002). CIPRO can be found in pharmaceutical waste waters as well as in hospital effluents (Harris et al. 2013; Vasconcelos et al. 2009b) and surface waters (often in the pharmaceutically active form) since this antibiotic is excreted during human therapy (Gad-Allah et al. 2011; Paul et al. 2007; Tokumura et al. 2011; Vasconcelos et al. 2009a, b).

Advanced oxidation processes (AOPs) are known as efficient, relatively low cost and easy to operate technologies that could be coupled with biological or traditional physicochemical processes for waste water treatment. Different AOPs have been already applied for degradation of the CIPRO antibiotic, such as ozonation (Sui et al. 2012), photocatalysis (El-Kemary et al. 2010; Van Doorslaer et al. 2011) and photo-Fenton process (Perini et al. 2013). However, most of these studies have been performed in batch or semibatch reactors; to

the best of our knowledge no reference to continuous flow treatment of CIPRO-contaminated water can be found in the literature.

From the above, the photo-Fenton process (named after the Fenton's reaction following the 1894 studies of Henry Fenton, on the oxidation reaction of tartaric acid (Fenton 1894)) consists on the generation of highly reactive hydroxyl radicals ($HO^{\bullet}$) from a mixture of hydrogen peroxide (H_2O_2) and Fe^{2+} ions at low pH (2–3), as shown in Eq. (1) (Herney-Ramirez et al. 2010; Ortega-Liébana et al. 2012; Punzi et al. 2012; Tokumura et al. 2011).

$$Fe^{2+} + H_2O_2 \rightarrow Fe^{3+} + OH^- + HO^{\bullet} \quad (1)$$

An optimized excess of H_2O_2 initiates the regeneration of Fe^{3+} into Fe^{2+} species—Eqs. (2) and (3). However, the amount of H_2O_2 in excess should be finely controlled since the H_2O_2 concentration cannot be far above its optimal; otherwise, termination by reaction with excess of hydroxyl radicals can occur—Eqs. (4) and (5) (Herney-Ramirez et al. 2010).

$$Fe^{3+} + H_2O_2 \rightleftharpoons Fe\text{-}OOH^{2+} + H^+ \quad (2)$$

$$Fe\text{-}OOH^{2+} \rightarrow Fe^{2+} + HO_2^{\bullet} \quad (3)$$

$$H_2O_2 + HO_2^{\bullet} \rightarrow HO_2^{\bullet} + H_2O \quad (4)$$

$$HO_2^{\bullet} + HO^{\bullet} \rightarrow H_2O + O_2 \quad (5)$$

When ultraviolet or visible light is used to assist the Fenton process, in what is known as the photo-Fenton process, there is a faster regeneration of Fe^{3+} into Fe^{2+} species—by Eq. (6) or by accelerating the reaction in Eq. (3)—and, as consequence, the normal cycle of the Fenton reaction is restarted (Herney-Ramirez et al. 2010; Tokumura et al. 2011).

$$Fe^{3+} + OH^- \rightarrow Fe^{2+} + HO^{\bullet} \quad (6)$$

Although the homogeneous photo-Fenton process has proved to be highly efficient for the degradation of several pollutants, there are several concerns when using iron salts as source of Fe^{2+} species, such as the generation of sludge wastes when the pH is increased after the treatment to precipitate the iron species. Iron-based heterogeneous catalysts have been developed in the last decades aiming to avoid the following: (1) high concentrations of iron species in the treated waters (the European Union standards for discharge of treated waters being 2.0 mg Fe L^{-1}), (2) the loss of catalyst, as well as (3) the sludge produced in the homogeneous process. The resulting system is known as photo-Fenton-like process (or heterogeneous photo-Fenton process) (Cong et al. 2012; Guo et al. 2010; Narayani et al. 2013; Patra et al. 2012; Soon and Hameed 2011; Zhu et al. 2012) and has been considered a promising alternative to overcome the main problems associated to the homogeneous route. Heterogeneous catalysts can be implemented in continuous flow reactors and, in particular, iron-based magnetic nanoparticles (MNP) have recently gained major relevance as catalysts of the photo-Fenton-like process since they can be used in slurry operation and easily separated from the treated water by an external magnetic field (Fu and Wang 2011; Guo et al. 2011; Liu et al. 2012; Narayani et al. 2013; Variava et al. 2012).

In order to make this process feasible for the treatment of high volumes of waste waters, as in the case of industrial or municipal effluents, the understanding of the effect of the main operating variables on the degradation of the target pollutants in the continuous regime is mandatory. The aim of this study is to study the influence of operating conditions on the continuous flow photo-Fenton treatment of CIPRO-contaminated water under simulated solar light, to select reference conditions for the photo-Fenton-like experiments with MNP prepared by chemical co-precipitation. The production of MNP was undertaken using the NETmix reactor, a proprietary rapid mixing technology developed at the University of Porto (Lopes et al. 2005). The NETmix reactor was previously proven successful for the co-precipitation synthesis of hydroxyapatite nanoparticles (Gomes et al. 2009) and, in the present work, it was used for the synthesis of magnetite (Fe_3O_4) by co-precipitation of two different iron precursors.

Experimental

Materials and reagents

Photo-Fenton experiments were performed using iron sulphate heptahydrate (99.5 %, Merck), ciprofloxacin (≥98 %, Fluka) and hydrogen peroxide (30 %, Fluka Analytical). Sodium sulphite anhydrous (≥98 %, Fluka) was used to stop the reaction when collecting the samples. Sulphuric acid (95–98 %, Sigma-Aldrich) and sodium hydroxide (97 %, Sigma-Aldrich) were used for pH adjustment. Acetonitrile (high-performance liquid chromatography (HPLC) grade, VWR), sodium hydrogen phosphate (≥99.0 %, Fluka Analytical), phosphoric acid (85.4 %, Fisher Scientific UK) and ultra-pure water (Direct-Q Millipore system) were used for HPLC analysis. Ammonium acetate (99 %, Fluka), acetic acid (99.8 %, Fluka), ascorbic acid (99 %, Sigma-Aldrich) and 1,10-phenantroline (≥99 %, Sigma-Aldrich) were used for the spectrophotometric measurement of dissolved iron.

Synthesis of MNP was done using iron(III) chloride hexahydrate (97 %, Sigma-Aldrich), iron(II) chloride tetrahydrate (99 %, Sigma-Aldrich), ammonium hydroxide solution (28–

30 %, Sigma-Aldrich) and sodium citrate tribasic dehydrate (99 %, Sigma-Aldrich).

Synthesis and characterization of magnetic nanoparticles

A stock solution of 0.250 mol L^{-1} iron(III) chloride and 0.125 mol L^{-1} iron(II) chloride was prepared using deoxygenated distilled water (solution A). Another stock solution, consisting of 2.50 mol L^{-1} ammonia was prepared by diluting a concentrated solution (solution B). Both solutions were prepared the earliest 24 h prior to the production run and kept under nitrogen atmosphere. Just before the production, trisodium citrate was dissolved in solution A to yield 0.02 mol L^{-1} citrate concentration.

MNP were then produced by pumping 500 mL of each solution at a total flow rate of 860 mL min^{-1} through the NETmix reactor (coupled to two Ismatec BVP Z pump drives with Z040 pump head). The resulting black dispersion was mixed for 10 min under nitrogen atmosphere to eliminate any possible unreacted iron and then centrifuged until the supernatant solution was clear. The supernatant solution was discarded and the precipitate was dispersed in deoxygenated distilled water by sonication. The cleaning run involving centrifugation and dispersion was repeated three times to achieve >99 % product purity. The final dispersion was spray-dried (on a Buchi Mini spray dryer B290) and kept under nitrogen atmosphere until used. The spray-dried powder was analysed by scanning electron microscopy (SEM) using a Phenom World Pro desktop SEM. MNP were re-dispersed in water prior to usage in photo-Fenton-like experiments and dynamic light scattering (DLS) analysis was performed in a Malvern Zeta Sizer Nano ZS equipment.

Photo-Fenton experiments

The continuous flow photo-Fenton system used for the degradation of CIPRO is illustrated in Fig. 1. A 9.5-mL glass reactor (E), with an inlet tube connected to a distilled water reservoir (A) and a second inlet tube connected to a reservoir containing a mixture of the catalyst and 10 mg L^{-1} of the CIPRO solution (C), was placed inside a solar simulator (G, Solarbox Model 1500e, CO.FO.MEGRA). In a typical experiment, before turning on the lamp (F), the reactor was filled up by means of a peristaltic pump (D) with the CIPRO solution mixed with the catalyst, and the system was stabilized during 25 min in dark conditions. Then, the flow from the reservoir filled with water (A) was replaced by the flow from a reservoir containing the H_2O_2 solution (B) and the lamp was immediately turned on. The continuous flow catalytic experiments were performed during 25 min, this period being enough to reach steady state (SS) conditions. Samples were periodically withdrawn from the reactor outlet tube for analysis and sodium sulphite immediately added to stop the reaction by consumption of the H_2O_2 remaining in the sample.

The effect of several key operating parameters on CIPRO degradation were studied, such as H_2O_2 (0–2.50 mM) and Fe^{2+} (0–10 mg L^{-1}) concentrations, as well as the initial pH (2.8–10), irradiance (I, up to 750 W m^{-2}) and residence time (τ, from 0.13 to 3.4 min), as summarized in Table 1. CIPRO conversion at SS ($X_{CIPRO,SS}$) was considered as the average conversion obtained between 20 and 25 min of irradiation.

In the photo-Fenton-like experiments, Fe^{2+} was replaced by a given amount of the magnetically recoverable catalyst (corresponding to 4.0 mg Fe L^{-1}).

Analytical techniques

The CIPRO concentration was determined with a Hitachi Elite LaChrom system equipped with a diode array detector (L-2450), a solvent delivery pump (L-2130) and a Hydrosphere C18 column (250 mm×4.60 mm i.d., 5 μm, YMC Europe GmbH). An isocratic method set at a flow rate of 1 mL min^{-1} was used with the eluent consisting of 85 % of 20 mM NaH_2PO_4, adjusted to pH 2.8 with phosphoric acid, and 15 % of acetonitrile. The concentration of dissolved iron was analysed colorimetrically according to ISO 6332:1988, by measuring the absorbance at 510 nm with an UV–Vis Jasco V-560 spectrophotometer.

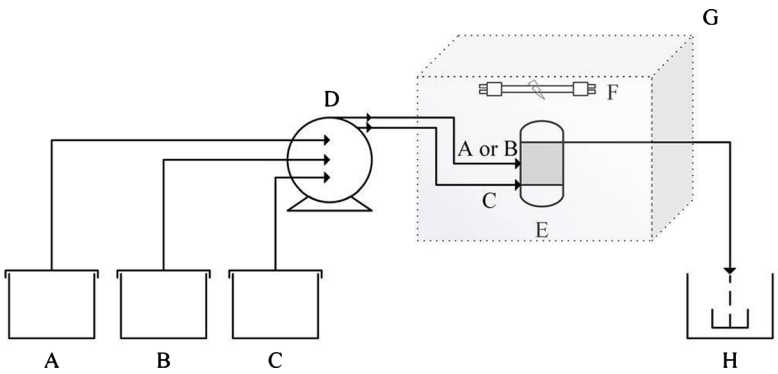

	Description
A	Water Reservoir
B	H_2O_2 Reservoir
C	CIPRO + Catalyst Reservoir
D	Peristaltic Pump
E	Photocatalytic Reactor
F	Irradiance Source
G	Solar Simulator
H	Reaction Drain

Fig. 1 Schematic view of the experimental setup

Table 1 Experimental conditions employed in continuous flow homogeneous photo-Fenton (using Fe^{2+}) and photo-Fenton like (using MNP) processes and respective H_2O_2/Fe^{2+} molar ratio, in terms of H_2O_2 and Fe^{2+} concentrations, as well as initial pH, irradiance (I) and residence time (τ)

$[H_2O_2]$ (mM)	$[Fe^{2+}]$ (mg L^{-1})	pH	I (W m^{-2})	τ (min)	H_2O_2/Fe^{2+} (molar ratio)
0	2.0	2.8	500	1.8	–
0.075	2.0	2.8	500	1.8	2.1
0.15	2.0	2.8	500	1.8	4.2
0.30	2.0	2.8	500	1.8	8.4
0.60	2.0	2.8	500	1.8	17
1.25	2.0	2.8	500	1.8	35
2.50	2.0	2.8	500	1.8	70
2.50	**0**	2.8	500	1.8	–
2.50	**0.07**	2.8	500	1.8	1,995
2.50	**0.5**	2.8	500	1.8	279
2.50	**1.0**	2.8	500	1.8	134
2.50	**4.0**	2.8	500	1.8	35
2.50	**10**	2.8	500	1.8	14
2.50	2.0	**6.8**	500	1.8	70
2.50	2.0	**10**	500	1.8	70
2.50	2.0	2.8	**0**	1.8	70
2.50	2.0	2.8	**250**	1.8	70
2.50	2.0	2.8	**500**	1.8	70
2.50	2.0	2.8	**750**	1.8	70
2.50	2.0	2.8	500	**0.13**	70
2.50	2.0	2.8	500	**0.42**	70
2.50	2.0	2.8	500	**0.63**	70
2.50	2.0	2.8	500	**0.93**	70
2.50	2.0	2.8	500	**3.4**	70
0	4.0 (MNP)	6.8	500	1.8	–
1.25	4.0 (MNP)	6.8	500	1.8	17
2.50	4.0 (MNP)	6.8	500	1.8	35
2.50	**0 (MNP)**	6.8	500	1.8	–
2.50	**2.0 (MNP)**	6.8	500	1.8	70
2.50	4.0 (MNP)	**2.8**	500	1.8	35
2.50	4.0 (MNP)	**10**	500	1.8	35
2.50	4.0 (MNP)	6.8	**0**	1.8	35
0	0	6.8	500	1.8	–

Bold parameters in a column means a set of experiments performed varying the respective parameter while keeping the others constant

Results and discussion

Homogeneous photo-Fenton process

The optimization of the homogeneous photo-Fenton process for the degradation of CIPRO under continuous flow conditions must consider several parameters. In Fig. 2, the influence of such parameters on the SS conversion of CIPRO can be assessed, namely the concentrations of Fe^{2+} (Fig. 2a) and H_2O_2 (Fig. 2b), the initial pH (Fig. 2c, d at 2.0 and 0.07 mg L^{-1} of dissolved iron, respectively), the residence time (τ, Fig. 2e) and the irradiance (I, Fig. 2f). Each parameter was tested independently (i.e. while keeping the others constant, in general at 2.0 mg L^{-1} of Fe^{2+}, 2.50 mM of H_2O_2, pH of 2.8, 1.8 min of τ and 500 W m^{-2} of I). In these figures, each data point corresponds to the result obtained in SS conditions when running a single experiment.

The influence of $[Fe^{2+}]$ on CIPRO conversion (Fig. 2a) shows that an increase up to 4.0 mg L^{-1} of the Fe^{2+} species has a positive effect on the CIPRO degradation. Above this concentration, CIPRO conversion is not affected. In addition, the pH of the final solution was similar to that of the initial one. Different H_2O_2 concentrations were tested by setting the initial Fe^{2+} concentration at 2.0 mg L^{-1} (corresponding to the maximum threshold of iron species allowed by the Portuguese legislation for discharge of treated waters—Decreto-Lei 236/98). In Fig. 2b, it is possible to observe that CIPRO conversion increases with H_2O_2 concentration up to 0.30 mM of H_2O_2 because more radicals are formed and effectively used in the reaction as the oxidant concentration increases. For higher H_2O_2 concentrations, the CIPRO conversion remains constant. The H_2O_2 concentration was maintained at 2.50 mM in the following experiments since an excess of H_2O_2 could regenerate Fe^{3+} to Fe^{2+}, as described previously, when other conditions are employed, and because the excess of hydroxyl radicals is not negatively affecting the CIRPO conversion. Even so, for scaled-up processes, the H_2O_2 concentration could be reduced to avoid non-efficient use of H_2O_2 and, thus, to decrease the operating costs of the process.

There are large discrepancies in reported optimal molar ratio of H_2O_2 to Fe^{2+} in photo-Fenton processes mostly due to the different organic charge of the waste waters treated and to different methods of determining this optimal dosage (Deng and Englehardt 2006). Perini et al. (2013) reported the photo-Fenton degradation of ciprofloxacin using H_2O_2/Fe^{2+} molar ratio of around 40. Bobu et al. (2013) have varied this ratio between 13.3 and 100 (at pH 3), the optimal value that maximized CIPRO conversion and total organic carbon removal being found for a H_2O_2/Fe^{2+} molar ratio of 20. A wide range of H_2O_2/Fe^{2+} molar ratio was studied in the present work. For instance, this ratio was changed between 0 and 70 when the experiments were performed at different H_2O_2 concentrations (Table 1).

It is well known that the Fenton reaction performs better at acidic medium (pH between 2 and 3), preventing the precipitation of iron and promoting the formation of photo-active Fe^{2+} species (Carra et al. 2013). It has been also reported that in the Fenton process the influence of the pH on the CIPRO oxidation reaction depends on the Fe^{2+} concentration (Parojčić et al. 2011). In this context, the influence of the initial pH was studied at two Fe^{2+} concentrations, namely 0.07 and 2.0 mg L^{-1}. At 2.0 mg L^{-1} of Fe^{2+} (Fig. 2c), the

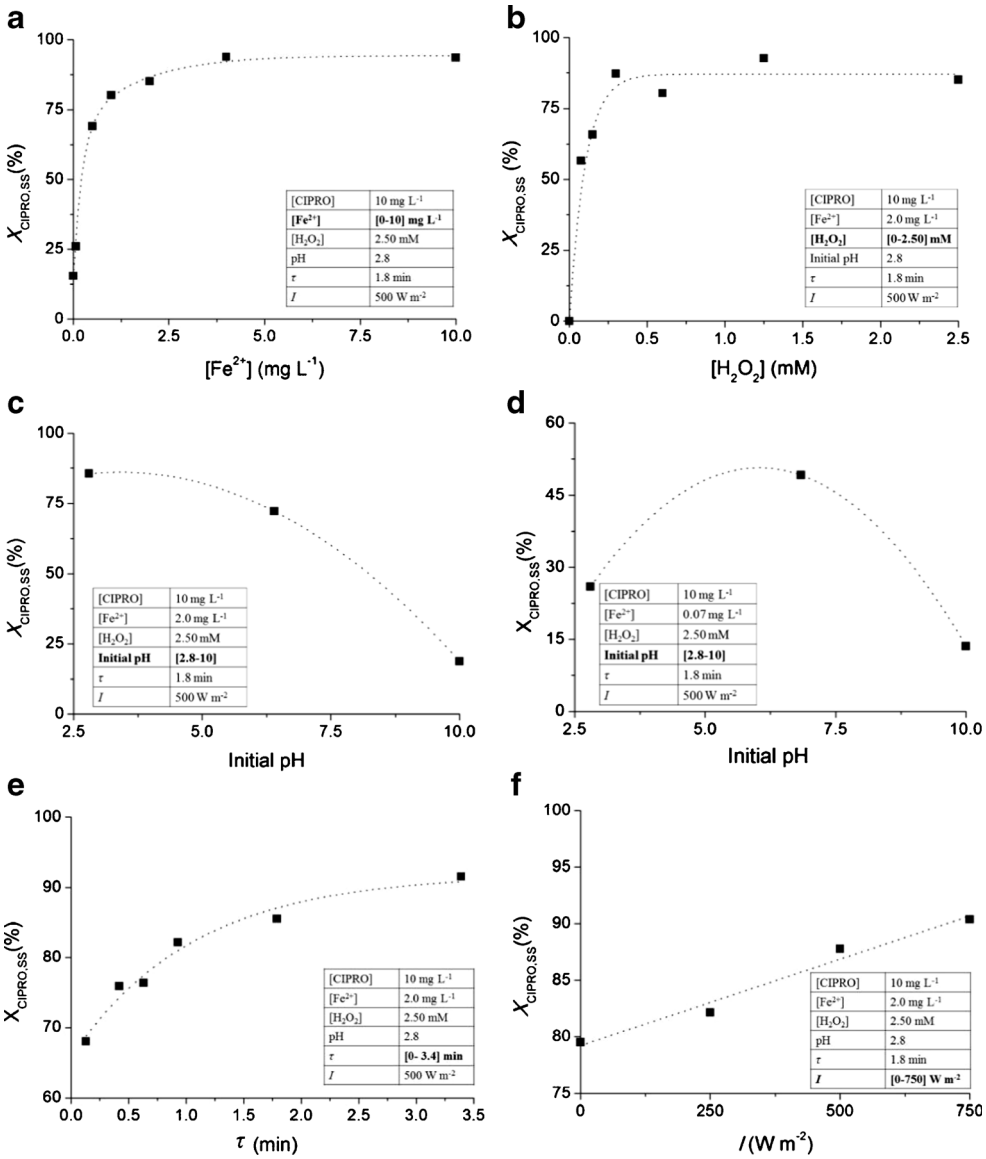

Fig. 2 Effect of operating parameters on the steady state conversion of CIPRO: **a** Fe^{2+} concentration (in milligram per litre); **b** H_2O_2 concentration (in millimolar); **c** pH for 2.0 mg L^{-1} of Fe^{2+}; **d** pH for 2.0 and 0.07 mg L^{-1} of Fe^{2+}; **e** residence time, τ, and **f** irradiance, I, when changing one variable at a time

homogeneous photo-Fenton process performs better at acidic pH (2.8), the efficiency decreasing gradually when increasing the initial pH (to natural, 6.8, or alkaline, 10). However, at the lowest Fe^{2+} concentration tested (0.07 mg L^{-1}), Fig. 2d shows that the efficiency of the photo-Fenton process is the highest at natural pH (pH=6.8).

It is known that the presence of iron species and the pH of the solution have influence on the solubility of CIPRO, as well as on the form as this antibiotic exist in the solution, influencing the CIPRO degradation rate (An et al. 2010; Carabineiro et al. 2012; Parojčić et al. 2011). The pK_a values for CIPRO are 5.90±0.15 (for the carboxylic acid group) and 8.89±0.11 (for the basic-N-moiety) and therefore it can exist as cation, anion and zwitterion (Drakopoulos and Ioannou 1997). The highest conversion observed at pH 6.8 when low concentration of Fe^{2+} (0.07 mg L^{-1}) is used can be related to the formation of CIPRO–iron complex, avoiding the precipitation of the metal and increasing the solubility of the antibiotic (Parojčić et al. 2011). On the other hand, when a Fe^{2+} initial concentration of 2.0 mg L^{-1} was used (corresponding to a near to 30-fold increase in Fe^{2+} concentration), the decrease of CIPRO removal efficiency with increasing pH should be attributed to the precipitation of iron as well as to a decrease in CIPRO solubility (Parojčić et al. 2011).

The τ of the solution in the reactor was varied between 0.13 and 3.4 min (Fig. 2e). CIPRO conversion reaches ca. 68 % at 0.13 min (the lowest τ), near 85 % at 1.8 min, and increases up to ca. 90 % at 3.4 min (the highest τ). The τ was set at 1.8 min in the following experiments. This τ allows high CIPRO conversions and assures complete mixing of the catalyst

during photo-Fenton-like experiments ("Photo-Fenton like process" section) that is not observed when lower flow rates (higher τ) are used.

Finally, in order to understand the influence of the irradiance (I) on CIPRO conversion, homogeneous photo-Fenton experiments were conducted under different irradiances. An experiment in the absence of light (Fenton process) was also performed. Figure 2f shows that at such conditions CIPRO conversion increases linearly with I. Aiming real-scale technological applications, the continuous flow system must mimic natural conditions to avoid the increase of associated costs. Therefore, an I of 500 W m^{-2} was chosen with the aim to simulate the typical solar irradiation conditions on Mediterranean countries (Šúri et al. 2007).

The degradation of CIPRO using the homogeneous photo-Fenton process was already reported in literature. In general, the studies were performed using batch reactors, typically at acidic pH (3.0–4.5 pH), a wide range of H_2O_2 concentration (1.5–10 mM) and relatively high concentration of CIPRO (15–50 mg L^{-1}). For instance, the CIPRO conversions were lower than 20 % at 10 min in the work of Perini et al. (2013) and found as high as 40 % in 5 min by Bobu et al. (2013). For very low concentrations of CIPRO (<0.002 mg L^{-1}) in effluents from a municipal wastewater treatment plant (together with around 60 other pollutants), the conversion after the photo-Fenton treatment (in a batch pilot compound parabolic collector solar plant) was 65 and 50 %, respectively at acidic and natural pH, after 20 min (Klamerth et al. 2013).

In our study, using a CIPRO initial concentration of 10 mg L^{-1}, 1.8 min of τ, 2.50 mM of H_2O_2 and 500 W m^{-2} of I, conversions of 85 and 73 % were achieved in a continuous flow homogeneous photo-Fenton system at pH of 2.8 and 6.8, respectively. Some preliminary photo-Fenton experiments were also performed at these conditions using a mixture consisting of CIPRO, trimethoprim and sulfamethoxazole antibiotics (10 mg L^{-1} for each and with a pH of 2.8), the conversion of these pollutants decreasing from 85, 87 and 65 %, when tested separately, to 54, 75 and 38 %, respectively, when tested together in the mixture. These results prove that the system could be scaled up to degrade mixtures of pollutants, after adjusting some of the operating parameters.

Photo-Fenton-like process

In the present work, the heterogeneous iron catalyst was obtained in the form of MNP that were synthesized by co-precipitation. The obtained magnetite particles (72 wt% of iron content) were analysed by SEM after the drying procedure used for the storage of these MNP, and also by DLS after dispersed in an aqueous solution for photo-Fenton-like experiments. MNP seem to agglomerate in the form of microparticles when they are dried (Fig. 3a) and easily dispersed to nanoscale in the aqueous solution, as shown by the respective particle size distribution (Fig. 3b). The dispersed MNP have ca. 20 nm average size with a narrow particle size distribution (as also observed by transmission electron microscopy, not shown).

The CIPRO conversion (X_{CIPRO}) for different initial pH in the presence of suspended MNP as catalyst for the photo-Fenton-like process is shown in Fig. 4a. It was found that the photo-Fenton-like reaction was positively influenced when using natural pH (6.8). Under these conditions, 50 % of CIPRO removal was achieved at SS, while only 25–30 % was obtained at the other pH (2.8 and 10), as also found in the homogeneous photo-Fenton experiments performed with a low concentration of Fe^{2+} (0.07 mg L^{-1} in Fig. 2d). In addition, the pH was similar from the beginning during the run where the initial pH was the lowest, and a decrease (to 9.0) was observed when using the highest initial pH.

In fact, although it has been long established in literature that homogeneous photo-Fenton and photo-Fenton-like processes are often more efficient at acidic pH (Alizadeh Fard et al. 2013; Devi et al. 2013; Fassi et al. 2013), some recent studies (Carra et al. 2013; Klamerth et al. 2013) have pointed out the possibility of efficient photo-Fenton reactions at natural pH conditions. The higher catalytic activity at natural pH is of interest for technological applications since the commonly

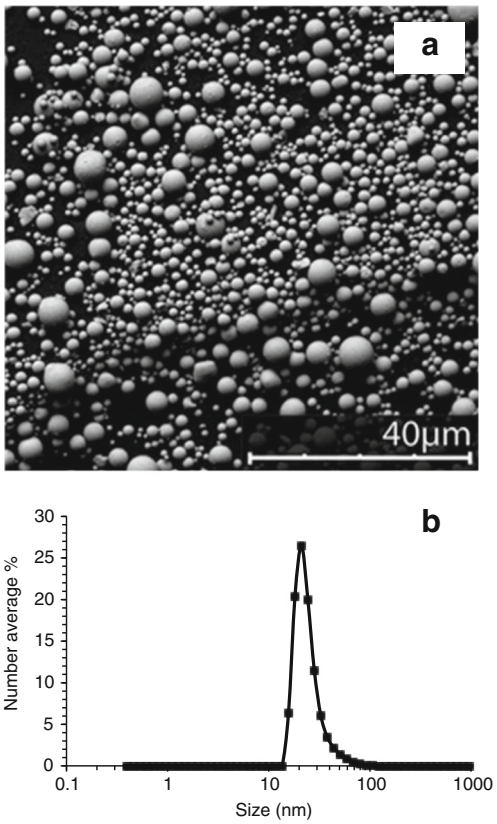

Fig. 3 MNP used in the photo-Fenton like process: **a** SEM micrograph of the spray-dried powder; **b** DLS analysis showing the average particle size distribution of the MNP dispersed in aqueous solution

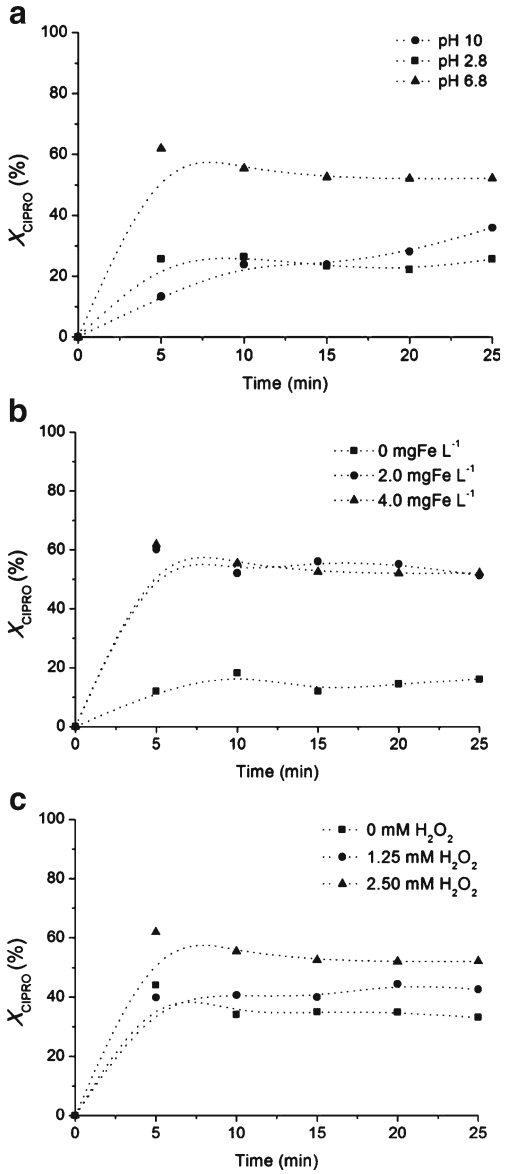

Fig. 4 Continuous flow photo-Fenton like experiments using MNP: **a** at different initial pH conditions, i.e. *square*, 2.8; *triangle*, 6.8; and *circle*, 10 (2.50 mM of H_2O_2, 4.0 mg Fe L^{-1} in the form of MNP); **b** different loads of MNP: *square*, 0 mg Fe L^{-1}; *circle*, 2.0 mg Fe L^{-1}; and *triangle*, 4.0 mg Fe L^{-1} (pH of 6.8 and 2.50 mM of H_2O_2); and **c** different H_2O_2 concentrations: *square*, 0 mM; *circle*, 1.25 mM; and *triangle*, 2.50 mM of H_2O_2 (pH of 6.8 and 4.0 mg Fe L^{-1} in the form of MNP). These experiments were performed using 1.8 min of τ and 500 W m^{-2} of I

required acidification of the reaction medium and the posterior neutralization of the treated water is not needed.

The influence of the MNP load and H_2O_2 concentration on the efficiency of CIPRO removal was also studied, as shown in panels b and c of Fig. 4, respectively. Figure 4b shows that the incorporation of MNP in the H_2O_2 photo-assisted process significantly increases the degradation of CIPRO in SS conditions (from 15 to 53 % for 0 to 2.0 mg Fe L^{-1}, respectively). Therefore, the non-catalytic process is not efficient and MNP can be successfully used to increase the process efficiency. Similar results for CIPRO degradation were observed when the load of MNP was increased from 2.0 to 4.0 mg Fe L^{-1}, suggesting that low loads of MNP are enough to drive the catalytic process.

Regarding the effect of the H_2O_2 concentration, Fig. 4c shows the results obtained in the absence of oxidant (0 mM of H_2O_2) and with two different H_2O_2 concentrations (1.25 and 2.50 mM, respectively). In SS conditions, it is possible to observe a gradual increase of the CIPRO degradation with the H_2O_2 concentration. For the homogeneous photo-Fenton process, an increase of the CIPRO conversion was observed when the H_2O_2 concentration was increased up to 0.5 mM, but similar CIPRO conversions were achieved in experiments with 1.25 and 2.50 mM of H_2O_2 (Fig. 2b), in contrast with the effect observed on the photo-Fenton-like process (Fig. 4c).

Therefore, natural pH, 2.50 mM of H_2O_2 and 2.0 mg Fe L^{-1} in the form of MNP are adequate conditions to achieve significant CIPRO degradation at SS. Complete CIPRO degradation could be probably achieved by optimizing the τ (lower τ results in higher CIPRO conversions) or the applied I (perhaps by implementing lamps with higher I than solar light), as observed for the homogeneous photo-Fenton process (panels e and f of Fig. 2, respectively).

Having into account the higher catalytic activity achieved in the photo-Fenton-like process under natural pH (triangle in Fig. 5), control reactions performed under natural pH have been summarized in Fig. 5, i.e. in the absence of catalyst (square) and in the absence of oxidant (circle), including also the results obtained in an experiment performed in the absence of light (inverted triangle) and with light only (diamond). In this figure, it is clear that catalytic CIPRO degradation can be greatly enhanced in the presence of light (55 %), which contrasts with the heterogeneous Fenton experiment performed in the dark, where negligible degradation of CIPRO is observed. Therefore, the irradiation is relevant in the photo-Fenton-like process with MNP. In addition, CIPRO degradation is very low (15 %) in the absence of the catalyst and in the presence of H_2O_2; in this case, the CIPRO degradation is only related to the action of light, since similar CIPRO conversions are obtained when using only photolysis. It is also noticed that MNP have photocatalytic activity even in the absence of H_2O_2 (35 % of CIPRO removal at SS conditions). Adsorption of CIPRO into MNP was never observed in the performed experiments.

The catalyst stability was examined by analysing the amount of iron species leached to the liquid phase in the experiment performed at natural pH, 2.50 mM of H_2O_2 and 2.0 mg Fe L^{-1} in the form of MNP, a very low amount being leached from the nanoparticles to the solution (0.07 mg L^{-1}). However, considering the relatively high catalytic activity achieved in the homogeneous photo-Fenton experiment with this concentration of Fe^{2+} (Fig. 2d), it is important to verify if

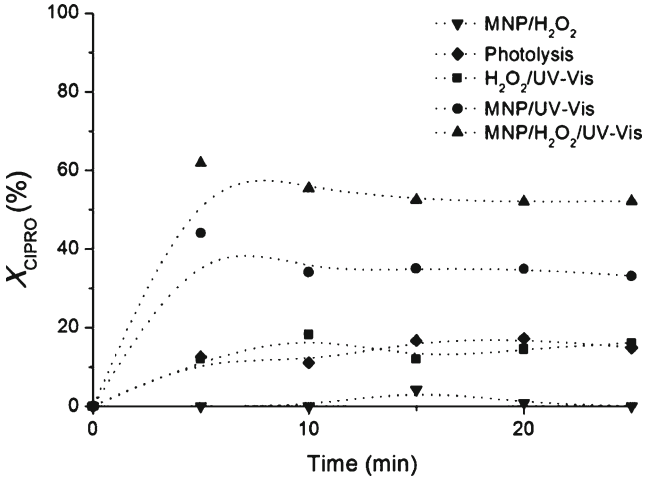

Fig. 5 Continuous flow experiments using MNP under different conditions: *diamond*, 500 W m^{-2} of *I*; *inverted triangle*, 4.0 mg Fe L^{-1} in the form of MNP and 2.50 mM of H_2O_2; *square*, 2.50 mM of H_2O_2 and 500 W m^{-2} of *I*; *circle*, 4.0 mg Fe L^{-1} in the form of MNP and 500 W m^{-2} of *I*; *triangle*, 4.0 mg Fe L^{-1} in the form of MNP, 2.50 mM of H_2O_2 and 500 W m^{-2} of *I*. These experiments were performed using 1.8 min of τ

MNP are acting as catalysts or if the photocatalytic activity is due to the presence of dissolved iron in the solution.

In fact, a significant percentage of the photocatalytic activity of MNP may be provided by the homogeneous phase due to leaching of iron species, since the CIPRO conversions obtained in homogeneous photo-Fenton and photo-Fenton-like experiments (with comparable amount of dissolved iron in aqueous phase) for a giving pH (2.8 and 6.8) are quite similar (Figs. 2d and 4a, respectively). Only in the case of the highest pH tested (10) these differences were more notorious, the photo-Fenton-like process presenting significantly higher CIPRO conversion.

Therefore, the present work demonstrates that aqueous solutions containing CIPRO can be treated by the photo-Fenton process under natural pH conditions and that in the case of the synthesized MNP a low leaching of iron species to the solution was observed, the amount of iron species dissolved being enough to drive the process. These MNP can be easily recovered after the treatment, by applying a magnetic field as shown in Fig. 6, and the treated water can be then discharged. Even so, the required concentration of dissolved iron species (0.07 mg L^{-1}) for degradation of CIPRO in the investigated photo-Fenton processes is far below the European Economic Community standards for discharge of treated waters (2.0 mg L^{-1}) and, therefore, a heterogeneous catalyst is not really required when treating effluents polluted with the CIPRO antibiotic. However, typical waste waters are often polluted with several organic pollutants and, therefore, the possible implementation of such MNP should be further investigated with actual waste waters where higher loads of catalyst will be probably required. In any case, capital and operating costs should be compared before any final decision. For the particular case of solar energy-driven systems (as in this particular case where solar energy was simulated), it is necessary to consider how the energy will be collected (Bolton et al. 2001). It is assumed that the capital cost of a solar collector is proportional to its area and, together with the first-order rate constant, it is possible to predict the system costs and an indication of the capital investment by using standard figures-of-merit that are useful tools when comparing advanced oxidation technologies.

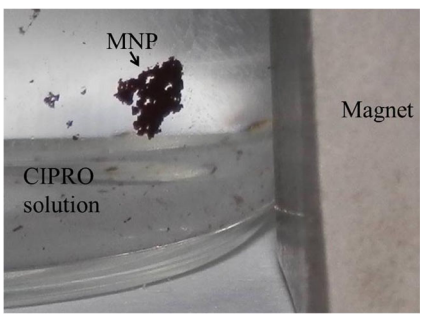

Fig. 6 Photograph of MNP separated by a magnetic field

Conclusions

The continuous flow photo-Fenton process is capable to degrade the CIPRO antibiotic. A higher efficiency was obtained at acidic pH (2.8), than at natural or alkaline pH (6.8 or 10, respectively), namely 85 % of ciprofloxacin conversion in steady state conditions (when employing 2.0 mg L^{-1} of Fe^{2+}, 2.50 mM of H_2O_2, 1.8 min of residence time and 500 W m^{-2} of *I*). For the photo-Fenton like process, using MNP, CIPRO removal was maximized at natural pH, instead of the acidic pH normally used as an optimized condition for the photo-Fenton reaction. The photocatalytic activity of the iron oxide MNP can be partially attributed to the homogeneous Fenton reaction occurring due to leaching of iron species to the solution. Nevertheless, this effect was more significant for pH 2.8 and 6.8. At higher pH values (pH 10) the heterogeneous photo-Fenton like process leads to higher CIPRO conversions than the respective homogenous reaction. The separation of the catalyst from the treated water was easily achieved by applying an external magnetic field that allows the use of the catalyst in consecutive reactions and avoids the production of sludge.

Acknowledgments Financial support was provided by projects PTDC/EQU-ERQ/123045/2010 and PTDC/EBB-EBI/103761/2008, and partially by LSRE/LCM LA financing Project PEst-C/EQB/LA0020/2013, financed by FEDER through COMPETE – Programa Operacional Factores de Competitividade, and by FCT - Fundação para a Ciência e a Tecnologia, for which the authors are thankful. AMTS acknowledges the FCT Investigator 2013 Programme (IF/01501/2013), with financing from the European Social Fund and the Human Potential

Operational Programme. CGS thanks FCT for the research grant SFRH/BPD/48777/2008.

References

Alizadeh Fard M, Torabian A, Bidhendi G, Aminzadeh B (2013) Fenton and photo-Fenton oxidation of petroleum aromatic hydrocarbons using nanoscale zero-valent iron. J Environ Eng 139:966–974

An T, Yang H, Li G, Song W, Cooper WJ, Nie X (2010) Kinetics and mechanism of advanced oxidation processes (AOPs) in degradation of ciprofloxacin in water. Appl Catal B Environ 94:288–294

Baquero F, Martínez J-L, Cantón R (2008) Antibiotics and antibiotic resistance in water environments. Curr Opin Biotechnol 19:260–265

Batt AL, Bruce IB, Aga DS (2006) Evaluating the vulnerability of surface waters to antibiotic contamination from varying wastewater treatment plant discharges. Environ Pollut 142:295–302

Bobu M, Yediler A, Siminiceanu I, Zhang F, Schulte-Hostede S (2013) Comparison of different advanced oxidation processes for the degradation of two fluoroquinolone antibiotics in aqueous solutions. J Environ Sci Health A Tox Hazard Subst Environ Eng 48:251–262

Bolton JR, Bircher KG, Tumas W, Tolman CA (2001) Figures-of-merit for the technical development and application of advanced oxidation technologies for both electric- and solar-driven systems. Pure Appl Chem 73:627–637

Carabineiro SAC, Thavorn-amornsri T, Pereira MFR, Serp P, Figueiredo JL (2012) Comparison between activated carbon, carbon xerogel and carbon nanotubes for the adsorption of the antibiotic ciprofloxacin. Catal Today 186:29–34

Carra I, Casas López JL, Santos-Juanes L, Malato S, Sánchez Pérez JA (2013) Iron dosage as a strategy to operate the photo-Fenton process at initial neutral pH. Chem Eng J 224:67–74

Cong Y, Li Z, Zhang Y, Wang Q, Xu Q (2012) Synthesis of α-Fe_2O_3/TiO_2 nanotube arrays for photoelectro-Fenton degradation of phenol. Chem Eng J 191:356–363

Deng Y, Englehardt JD (2006) Treatment of landfill leachate by the Fenton process. Water Res 40:3683–3694

Devi LG, Munikrishnappa C, Nagaraj B, Rajashekhar KE (2013) Effect of chloride and sulfate ions on the advanced photo Fenton and modified photo Fenton degradation process of Alizarin Red S. J Mol Catal A Chem 374–375:125–131

Drakopoulos AI, Ioannou PC (1997) Spectrofluorimetric study of the acid–base equilibria and complexation behavior of the fluoroquinolone antibiotics ofloxacin, norfloxacin, ciprofloxacin and pefloxacin in aqueous solution. Anal Chim Acta 354:197–204

El-Kemary M, El-Shamy H, El-Mehasseb I (2010) Photocatalytic degradation of ciprofloxacin drug in water using ZnO nanoparticles. J Lumin 130:2327–2331

Fassi S, Djebbar K, Bousnoubra I, Chenini H, Sehili T (2013) Oxidation of bromocresol green by different advanced oxidation processes: Fenton, Fenton-like, photo-Fenton, photo-Fenton-like and solar light. Comparative study. Desalination Water Treat 1–8, doi: 10.1080/19443994.2013.809971

Fenton HJH (1894) LXXIII.-Oxidation of tartaric acid in presence of iron. J Chem Soc Trans 65:899–910

Fu Y, Wang X (2011) Magnetically separable $ZnFe_2O_4$-graphene catalyst and its high photocatalytic performance under visible light irradiation. Ind Eng Chem Res 50:7210–7218

Gad-Allah TA, Ali MEM, Badawy MI (2011) Photocatalytic oxidation of ciprofloxacin under simulated sunlight. J Hazard Mater 186:751–755

Gomes PJ, Silva VMTM, Quadros PA, Dias MM, Lopes JCB (2009) A highly reproducible continuous process for hydroxyapatite nanoparticles synthesis. J Nanosci Nanotechnol 9:3387–3395

Guo L, Chen F, Fan X, Cai W, Zhang J (2010) S-doped α-Fe_2O_3 as a highly active heterogeneous Fenton-like catalyst towards the degradation of acid orange 7 and phenol. Appl Catal B Environ 96:162–168

Guo R, Fang L, Dong W, Zheng F, Shen M (2011) Magnetically separable $BiFeO_3$ nanoparticles with a γ-Fe_2O_3 parasitic phase: controlled fabrication and enhanced visible-light photocatalytic activity. J Mater Chem 21:18645–18652

Harris S, Morris C, Morris D, Cormican M, Cummins E (2013) The effect of hospital effluent on antimicrobial resistant *E. coli* within a municipal wastewater system. Environ Sci Process Impacts 15:617–622

Herney-Ramirez J, Vicente MA, Madeira LM (2010) Heterogeneous photo-Fenton oxidation with pillared clay-based catalysts for wastewater treatment: a review. Appl Catal B Environ 98:10–26

Klamerth N, Malato S, Agüera A, Fernández-Alba A (2013) Photo-Fenton and modified photo-Fenton at neutral pH for the treatment of emerging contaminants in wastewater treatment plant effluents: a comparison. Water Res 47:833–840

Kolpin DW, Furlong ET, Meyer MT, Thurman EM, Zaugg SD, Barber LB, Buxton HT (2002) Pharmaceuticals, hormones, and other organic wastewater contaminants in U.S. streams, 1999–2000: a national reconnaissance. Environ Sci Technol 36:1202–1211

Liu S-Q, Feng L-R, Xu N, Chen Z-G, Wang X-M (2012) Magnetic nickel ferrite as a heterogeneous photo-Fenton catalyst for the degradation of rhodamine B in the presence of oxalic acid. Chem Eng J 203:432–439

Lopes JCB, Laranjeira PE, Dias MM, Martins AA (2005) Network mixer and related mixing process. PCT/IB2005/000647, February 2005. European Patent EP172643 B1, October 2008

Narayani H, Arayapurath H, Shukla S (2013) Using Fenton-reaction as a novel approach to enhance the photocatalytic activity of TiO_2-γ-Fe_2O_3 magnetic photocatalyst undergoing photo-dissolution process without silica interlayer. Catal Lett 143:807–816

Oliphant CM, Green GM (2002) Quinolones: a comprehensive review. Am Fam Physician 65:455–464

Onesios K, Yu J, Bouwer E (2009) Biodegradation and removal of pharmaceuticals and personal care products in treatment systems: a review. Biodegradation 20:441–466

Ortega-Liébana MC, Sánchez-López E, Hidalgo-Carrillo J, Marinas A, Marinas JM, Urbano FJ (2012) A comparative study of photocatalytic degradation of 3-chloropyridine under UV and solar light by homogeneous (photo-Fenton) and heterogeneous (TiO_2) photocatalysis. Appl Catal B Environ 127:316–322

Parojčić J, Stojković A, Tajber L, Grbić S, Paluch KJ, Djurić Z, Corrigan OI (2011) Biopharmaceutical characterization of ciprofloxacin HCl–ferrous sulfate interaction. J Pharm Sci 100:5174–5184

Patra AK, Dutta A, Bhaumik A (2012) Highly ordered mesoporous TiO_2-Fe_2O_3 mixed oxide synthesized by sol–gel pathway: an efficient and reusable heterogeneous catalyst for dehalogenation reaction. ACS Appl Mater Interfaces 4:5022–5028

Paul T, Miller PL, Strathmann TJ (2007) Visible-light-mediated TiO_2 photocatalysis of fluoroquinolone antibacterial agents. Environ Sci Technol 41:4720–4727

Perini JAL, Perez-Moya M, Nogueira RFP (2013) Photo-Fenton degradation kinetics of low ciprofloxacin concentration using different iron sources and pH. J Photochem Photobiol A Chem 259: 53–58

Punzi M, Mattiasson B, Jonstrup M (2012) Treatment of synthetic textile wastewater by homogeneous and heterogeneous photo-Fenton oxidation. J Photochem Photobiol A Chem 248:30–35

Soon AN, Hameed BH (2011) Heterogeneous catalytic treatment of synthetic dyes in aqueous media using Fenton and photo-assisted Fenton process. Desalination 269:1–16

Sui M, Xing S, Sheng L, Huang S, Guo H (2012) Heterogeneous catalytic ozonation of ciprofloxacin in water with carbon nanotube supported manganese oxides as catalyst. J Hazard Mater 227–228:227–236

Šúri M, Huld TA, Dunlop ED, Ossenbrink HA (2007) Potential of solar electricity generation in the European Union member states and candidate countries. Sol Energy 81:1295–1305

Tokumura M, Morito R, Hatayama R, Kawase Y (2011) Iron redox cycling in hydroxyl radical generation during the photo-Fenton oxidative degradation: dynamic change of hydroxyl radical concentration. Appl Catal B Environ 106:565–576

Van Doorslaer X, Demeestere K, Heynderickx PM, Van Langenhove H, Dewulf J (2011) UV-A and UV-C induced photolytic and photocatalytic degradation of aqueous ciprofloxacin and moxifloxacin: reaction kinetics and role of adsorption. Appl Catal B Environ 101:540–547

Variava MF, Church TL, Harris AT (2012) Magnetically recoverable Fe_xO_y-MWNT Fenton's catalysts that show enhanced activity at neutral pH. Appl Catal B Environ 123–124:200–207

Vasconcelos TG, Henriques DM, König A, Martins AF, Kümmerer K (2009a) Photo-degradation of the antimicrobial ciprofloxacin at high pH: identification and biodegradability assessment of the primary by-products. Chemosphere 76:487–493

Vasconcelos TG, Kümmerer K, Henriques DM, Martins AF (2009b) Ciprofloxacin in hospital effluent: degradation by ozone and photoprocesses. J Hazard Mater 169:1154–1158

Yu JT, Bouwer EJ, Coelhan M (2006) Occurrence and biodegradability studies of selected pharmaceuticals and personal care products in sewage effluent. Agric Water Manag 86:72–80

Zhu LP, Bing NC, Wang LL, Jin HY, Liao GH, Wang LJ (2012) Self-assembled 3D porous flowerlike α-Fe_2O_3 hierarchical nanostructures: synthesis, growth mechanism, and their application in photocatalysis. Dalton Trans (Cambridge, England: 2003) 41: 2959–2965